

This is the peer reviewed version of the following article:

Mechanical performance and crack pattern analysis of aged Carbon Fabric Cementitious Matrix (CFRCM) composites / Signorini, Cesare; Nobili, Andrea; Falope, Federico O.. - In: COMPOSITE STRUCTURES. - ISSN 0263-8223. - 202:(2018), pp. 1114-1120. [10.1016/j.compstruct.2018.05.052]

Terms of use:

The terms and conditions for the reuse of this version of the manuscript are specified in the publishing policy. For all terms of use and more information see the publisher's website.

21/09/2024 11:49

(Article begins on next page)

Mechanical performance and crack pattern analysis of aged Carbon Fabric Cementitious Matrix (CFRCM) composites

Cesare Signorini^{a,*}, Andrea Nobili^b, Federico O. Falope^b

^a*Dipartimento di Scienze e Metodi dell'Ingegneria (DISMI), University of Modena and Reggio Emilia, Via Giovanni Amendola, 2, 42122 Reggio Emilia*

^b*Dipartimento di Ingegneria "Enzo Ferrari" (DIEF), University of Modena and Reggio Emilia, Via Pietro Vivarelli, 10, 41125 Modena*

Abstract

We discuss the effect of environmental exposure on mechanical performance of impregnated Carbon Fabric Reinforced Cementitious Matrix (CFRCM) composite. Following the recently published ICC-ES AC434 guidelines, mechanical performance of prismatic composite specimens is determined on the basis of tensile uni-axial tests. Exposure to saline and alkaline aqueous solutions is considered at 28- as well as 60-day curing time. Special emphasis is placed on crack pattern evaluation as a mean to gain better insight into matrix/fabric bond quality. To this aim, the evolution of the average crack spacing and of the average crack width is determined as a function of strain for all test environments and curing times. It is found that curing time plays a significant role in mitigating the detrimental effect of aggressive environments. Furthermore, the average crack spacing provides a very reliable measure of matrix/fabric bond degradation at all test stages.

Keywords: Durability; Textile reinforced mortar; Carbon fabric cementitious composite

1. Introduction

Continuous fibre composite materials have been actively investigated in the last three decades as effective materials for seismic retrofitting and strengthening. These lightweight and versatile composites can be grouped according to the organic/inorganic nature of the matrix, respectively FRP (Fibre Reinforced Polymers) and FRCM (Fabric Reinforced Cementitious Matrix) or TRC/TRM (Textile Reinforcement Concrete/Mortar). The reinforcement most commonly employed in FRP and FRCM consists of woven fabric (uni- or multi-axial)

*Corresponding author

Email address: cesare.signorini@unimore.it (Cesare Signorini)

9 wherein fibres are usually chosen according to their strength and **deformability**.
10 Fibres can be divided into conventional (steel and glass), high-modulus (typi-
11 cally aramidic, polyphenylenebenzobisoxazole (PBO) or carbon), low-modulus
12 (polypropylene) or natural (straw, hemp, cellulose, flax). Low-modulus and
13 natural fibres are more often employed in Fibre Reinforced Concrete (FRC) as
14 discrete randomly-distributed reinforcing elements [1]. FRP have been widely
15 investigated and adopted in engineering structures also in consideration of the
16 wide availability of design criteria in many national codes (for instance [2]).
17 However, FRP suffer from some severe drawbacks which hinder their general
18 applicability and prompt demand for new technologies [3]. FRCM composite
19 materials may be preferable owing to their composition, which appears compat-
20 ible with the traditional inorganic (brick/mortar, cement) substrate, to their
21 porosity, that warrants "breathability", to their resistance to **high tempera-**
22 **tures**. Nevertheless, the adoption of FRCM composite is hindered by the lack of
23 regulations. Recently, the International Code Council Evaluation Services (ICC-
24 ES) [4] and the International union of laboratories and experts in construction
25 materials, systems and structures (RILEM) [5] provided a backbone of regula-
26 tions to implement FRCM composite materials. Besides, FRCM suffers from
27 the lack of fabric-to-matrix adhesion, which leads to inconsistent performance
28 and telescopic failure [6].

29 Material durability is a critical issue whose deep understanding is required
30 before a material may undergo large scale application. Arboleda et al. [7, 8]
31 investigated durability of carbon and **PBO FRCM** systems. In [9], the mechan-
32 ical response of alkali-resistant glass (ARG) FRCM coupons after exposure to
33 saline and alkaline environment is considered. A similar analysis is presented in
34 [10] for several reinforcement fabrics in the alkaline environment. In [11, 12, 13]
35 glass fabric durability in the alkaline environment is assessed through pull-out,
36 tensile and bending tests. [14] **considers the crack pattern evolution in uni-axial**
37 **traction of low modulus woven polyethylene fabric and bonded AR-glass mesh**
38 **TRC composites**. In this paper, we investigate the effects of curing time and
39 aggressive environment exposure on the mechanical performance of C-FRCM.
40 According to the ICC guidelines, mechanical performance is assessed in uni-axial
41 traction of prismatic coupons. Particular emphasis is placed on crack pattern
42 evolution as a **means** to infer interphase bond quality.

43 **2. Materials and methods**

44 *2.1. Reinforcing fabric*

45 A commercially available square-grid bi-axial carbon fabric is adopted as the
46 reinforcing phase (Figure 1). This fabric is produced by weaving and thermo-
47 welding high-tenacity multi-filament carbon yarns. The mechanical properties
48 of the fabric are gathered in Table 1.

49 *2.2. Impregnating agent*

50 Fabrics are impregnated by immersion in a bi-component hybrid mineral/polymeric
51 adhesion promoter (hereafter "impregnating agent"). The mineral component

Characteristic	Unit	Value
Yarn count	tex	800
Specific weight per unit fabric area	g/m ²	200
Fabric specific weight	g/cm ³	1.78
Grid spacing (square grid side)	mm	8
Carbon fabric cross-sectional area (per unit width), A_f	mm ² /cm	0.56
Ultimate strength along the principal direction (epoxy impregnated)	N/cm	1800
Elastic modulus	GPa	240

Table 1: Carbon fabric mechanical properties (1 tex = 1 g/km)

Characteristic	Unit	Value
Adhesion to concrete	MPa	≥ 3
Flexural strength	MPa	≥ 5
Ultimate strain	mstrain	≥ 12
Flexural modulus	MPa	50

Table 2: Impregnating agent mechanical properties

52 acts as a filler and imparts superior resistance to the aggressive environments.
 53 The impregnated fabric is embedded in the cementitious matrix prior to set-
 54 ting of the polymeric phase (wet phase). The main mechanical and physical
 55 properties of the impregnating agent are reported in Table 2.

56 2.3. Inorganic matrix

57 A pre-mixed natural lime-based hydraulic mortar (NHL) is adopted as in-
 58 organic matrix and its main mechanical properties are presented in Table 3.
 59 This low-modulus mortar is especially designed to strengthen historical or aged
 60 masonry and it consistently develops high-quality bond with the impregnating
 61 agent.

62 2.4. Specimen manufacturing

63 Specimen manufacturing and testing are performed according to Annex A of
 64 [4]. Specimen preparation occurs on an individual basis in a specially designed

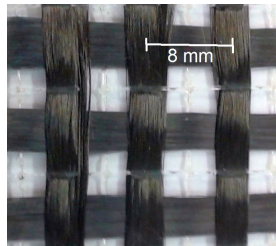


Figure 1: The multi-filament bi-axial carbon reinforcing fabric

Characteristic	Unit	Value
Density of the mixture	kg/m ³	1700
Mean compression strength after 28 days (UNI EN 12190)	MPa	≥ 6.5
Mean flexural strength after 28 days (UNI EN 196/1)	MPa	≥ 3
Support adhesion strength after 28 days	MPa	1
Water content	-	23%
Aggregate maximum size	mm	0.7
Longitudinal elastic modulus	GPa	11
Water vapor permeability μ	-	12

Table 3: Mortar properties provided by the producer (Brigliadori Fornace Calce).

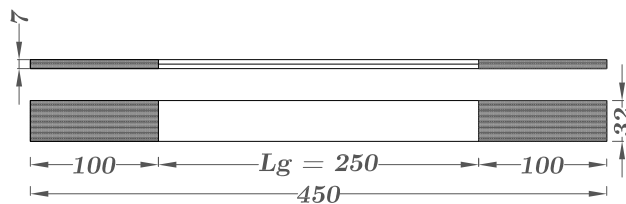


Figure 2: Coupon geometry (dimensions in *mm*)

65 modular polyethylene formwork, see [9, 3] for more details. The specimen ge-
66 ometry is illustrated in Figure 2 and, in conformity with the ICC guidelines [4],
67 specimen width is an integer multiple of the mesh size, namely $w_f = 320$ mm.
68 According to [2, §2.2.3.1], the laminate cross-sectional area is designed according
69 to the following expression:

$$A_f = \frac{T_x N_f}{10^4 \rho_f} w_s = 1.79 \text{ mm}^2 \quad (1)$$

70 In Eq.(1), $T_x = 800$ tex is the yarn count in the principal direction, $N_f =$
71 1.25 cm^{-1} is the number of yarns per unit length and $\rho_f = 1.78 \text{ g/cm}^3$ is the
72 density of the carbon fibre. In the following, strength values are conventionally
73 referred to this cross-sectional area.

74 As prescribed in [15, 16], moist-curing is carried out in a polypropylene bag
75 for 7 days to prevent differential shrinkage between the top surface, exposed
76 to air, and the bottom surface, in contact with the formwork. 28- and 60-day
77 curing is considered. 100 mm-long carbon fabric tabs are epoxy glued to the
78 specimens ends to accommodate for the testing machine grips. Cured specimens
79 are shown in Figure 3. The specimen gauge length (net of end tabs), L_g , is equal
80 to 250 mm. For statistical significance, a minimum of 5 specimens is considered
81 in every test group.

82 2.5. Aggressive environments

83 The following aggressive solutions are considered, according to the prescrip-
84 tions in [4]:

Test groups	Curing [days]	Exposure time [hrs]	Temperature		Ref.
			°C	F	
Control (CC28/CC60)	28/60	-	room		-
Saline (SW28/SW60)	28/60	1000	23 ± 1	73 ± 2	[4, Table 2]
Alkaline (AK28/AK60)	28/60	1000	23 ± 1	73 ± 3	[4, Table 2]

Table 4: Tested environments; room temperature is $21 \pm 2^\circ\text{C}$ (70 ± 3.6 F)

- 85 • a 3.5 %-weight saline solution that represents ocean water average salinity.
86 It is prepared dissolving pure sodium chloride into distilled water.
- 87 • an alkaline solution with pH= 10 (prescribed $\text{pH} \geq 9$). It is prepared
88 diluting in distilled water concentrated sodium hydroxide (NaOH, Sigma
89 Aldrich Inc.) until pH reaches the target value.

90 Specimens age in a Memmert HP110 climatic chamber at constant temperature
91 $T = 37.7^\circ\text{C}$ for 1000 hours [4]. The temperature in the chamber is double
92 checked by an independent recorder.

93 2.6. Curing time

94 In order to correlate the maturation grade of the hydraulic matrix [15] with
95 the loss of mechanical performance due to aging, 28 and 60-day curing is con-
96 sidered. Specimens groups and aging details are summarized in Table 4.

97 2.7. Testing procedure

98 Specimen performance is evaluated in uni-axial tensile tests through a In-
99 stron 5567 Universal Testing Machine (UTM), equipped with a 30 kN load cell
100 and wedge grips. Hinges warrant a uni-axial tensile stress state. Tests are carried
101 out under displacement control with nominal rate 0.5 mm/min (this translates
102 in terms of nominal axial strain as $\dot{\epsilon} = \dot{\delta}/L_g = 2$ mstrain/min).

103 2.8. Digital Image Correlation

104 As already pointed out in [17], strength curves and crack evolution should be
105 determined from actual specimen strain as opposed to imposed nominal strain.
106 Indeed, the former is affected by the contribution of wedge grip elongation



Figure 3: Two stages in specimen manufacturing: specimens cure in the modular formwork (left) and, after stripping, they are provided with end tabs (right).

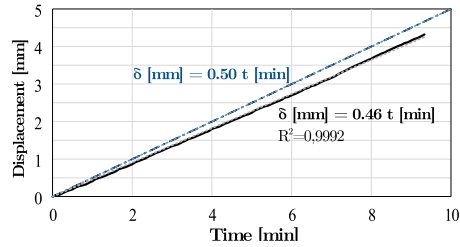


Figure 4: Nominal ramp (dotted line) vs. DIC acquired displacement data (solid line) and linear curve fitting expression

107 which is load dependent. To this aim, a Q400 Dantec Dynamics Digital Image
 108 Correlation (DIC) stereoscopic system is employed. Fig.4 compares the nominal
 109 ramp with the measured displacement as a function of time and it shows that a
 110 linear fitting provides good accuracy. Hereinafter, strain data are always given
 111 in terms of measured values.

112 3. Experimental results and discussions

113 3.1. Effects of curing time

114 Fig.5 illustrates the effect of curing time on the ultimate tensile strength
 115 and elongation for all specimen groups. It is observed that the small perform-
 116 ance increase, both in terms of strength and strain, associated with the control
 117 group has little statistical significance. Conversely, the important role played
 118 by curing time in reducing the performance decay associated with all aggressive
 119 environments is clearly defined. Table 5 gathers the percentage decay against
 120 the relevant control group. It shows that moving from 28 to 60-day curing time
 121 reflects on a decay in terms of mechanical properties going from 60 % to 32 %
 122 for the AK samples, and from 65 % to 39 % for the SW samples. A similar trend
 123 is observed in terms of ultimate strain and the overall pictures resembles what
 124 is found in [18, 19]. Indeed, curing time affects the matrix porosity which has a
 125 strong impact on the diffusion of aggressive agents.

126 3.2. Optical and SEM analysis

127 An optical analysis of 28-day cured specimens is presented in Fig.6 at 35x
 128 magnification. While the CC28 specimen shows a polished reflecting surface,
 129 SW28 and especially AK28 specimens are opaque and present diffuse abrasion
 130 and salt deposition. Fig.7 is a SEM investigation of the carbon fabric emerging
 131 from the failure surface of a AK28 specimen. It suggests that matrix degradation
 132 strongly weakens the fabric-to-mortar interface bond, as the carbon yarn surface
 133 appears mostly deprived of matrix patches.

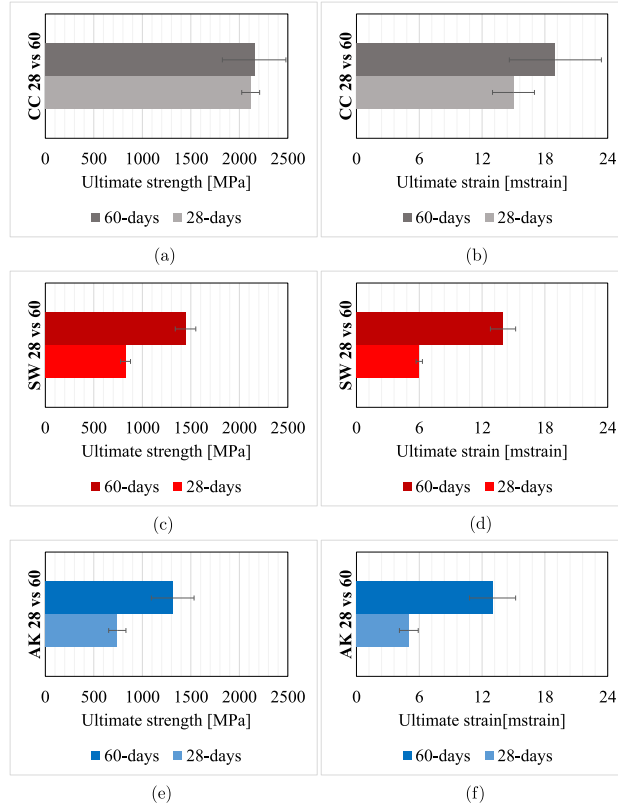


Figure 5: Bar-chart comparison of mean strength (left) and ultimate strain (right panel) at 28- and 60-day curing-times for all sample groups: (a, b) control (c, d) saline and (e, f) alkaline

134 *3.3. Crack pattern analysis*

135 Crack analysis is carried out to relate mechanical properties to the failure
 136 mechanism and to matrix deterioration. Indeed, crack spacing provides indirect
 137 evidence of interphase bond strength and it affects the apparent composite stiff-
 138 ness [20]. **A nice introduction to the significance and application of crack spacing**
 139 **measurement is given in [21, Chap.13]. It is important to observe that crack**
 140 **spacing may be adopted as a design parameter.** Besides, crack widening and
 141 diffusion clearly affects durability. Fig.8 shows a color map of the longitudinal
 142 displacement field for all test group at 28-day curing time ($\varepsilon = 5.5$ mstrain). The
 143 control group exhibits several small uniformly colored patches as an evidence of
 144 multiple small cracks developing throughout the specimen length. Conversely,
 145 the SW and AK groups show few large color patches, which indicate that dis-
 146 placement jumps are concentrated around a small number of wide cracks, with
 147 clear negative implications in terms of ductility as well as durability [22].

148 This qualitative picture is given a quantitative description in Fig.9, that

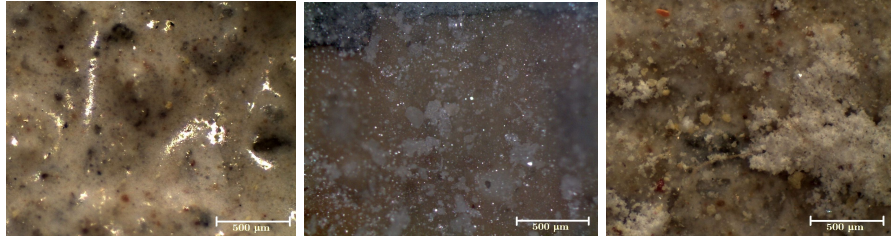


Figure 6: Optical microscopy investigation at 35x magnification of the mortar surface for CC28 (a), SW28 (b) and AK28 (c) specimens

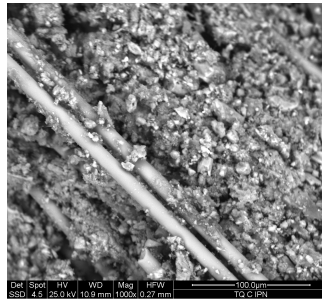


Figure 7: SEM magnification of the carbon fabric emerging from a AK28 failed specimen

149 plots the average crack spacing as well as the average crack width as a function
 150 of strain for AK, SW and CC and it compares 28-day with 60-day curing. **In**
 151 **general, crack spacing is a decreasing function of strain, until a saturation level**
 152 **is reached [14]. Conversely, crack width is found to almost linearly increase**
 153 **with strain.** Remarkably, the crack pattern development in the control group
 154 for 28- and 60-day curing time almost coincide. Conversely, AK and SW speci-
 155 mens display a marked contrast between 28- and 60-day curing, with the crack
 156 spacing being almost uniformly twice as large for the former compared to the
 157 latter and the crack width increasing at a much slower rate. However, despite
 158 this different evolution, the ultimate mean crack width $w_{cr,u}$ attained at failure
 159 appears similar for all test groups, as reported in Table 6. Such saturation crack
 160 width is located around the mean value $\mu(w_{cr,u}) = 185 \mu\text{m}$ with narrow stan-

Environment	Curing time [days]	Decay in strength [%]	Decay in strain [%]
AK	28	65	64
	60	39	33
SW	28	60	64
	60	32	28

Table 5: Performance decay of mechanical properties for 28- and 60-day curing times

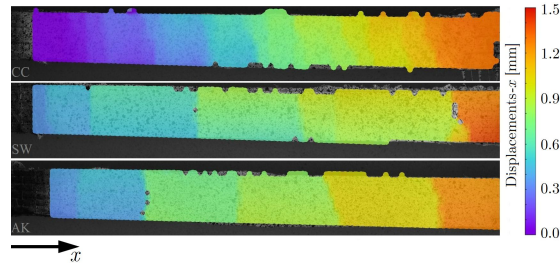


Figure 8: Longitudinal displacement field according to DIC at $\varepsilon = 5.5$ mstrain for all specimen groups at 28-day curing time

28-day curing	$w_{cr,u}$ [μm]	60-day curing	$w_{cr,u}$ [μm]
CC28	193	CC60	161
SW28	184	SW60	180
AK28	176	AK60	217

Table 6: Average crack width at failure for CC, SW and AK groups

161 dard deviation $\sigma(w_{cr,u}) = 18 \mu\text{m}$, that corresponds to a unexpectedly limited
 162 coefficient of variation, $CV \approx 10\%$. Thus, it appears that the saturation crack
 163 width is a characteristic parameter of this composite system [23, 6].

164 4. Conclusions

165 The effect of aggressive environment exposure on the mechanical perfor-
 166 mance of carbon fabric mortar composites is investigated, conforming to the
 167 recently proposed guidelines [4], through uni-axial traction tests. Carbon fabric
 168 is impregnated by a bi-component partly organic liquid agent. Strength curves,
 169 ultimate strength and elongation limits as well as crack pattern analysis are
 170 presented. The following points summarize the main findings:

- 171 • Environmental conditions heavily affect the expected performance and
 172 should be carefully taken into account for the computation of the design
 173 ultimate values [3]. The alkaline (typical of rural and industrial areas) and
 174 saline (seaside, waterfront areas, ports) environments are equally detri-
 175 mental and produce a strength reduction exceeding 60% of the control
 176 group at 28-day curing. Their action mainly targets the matrix and its
 177 bond formation capability.
- 178 • Long-term curing provides strong protection against aggressive attack and
 179 it should be carefully considered for laminates exposed to adverse envi-
 180 ronments. Indeed, a remarkable mitigation of performance degradation is
 181 observed at 60-day curing with the performance loss sitting below 40% of

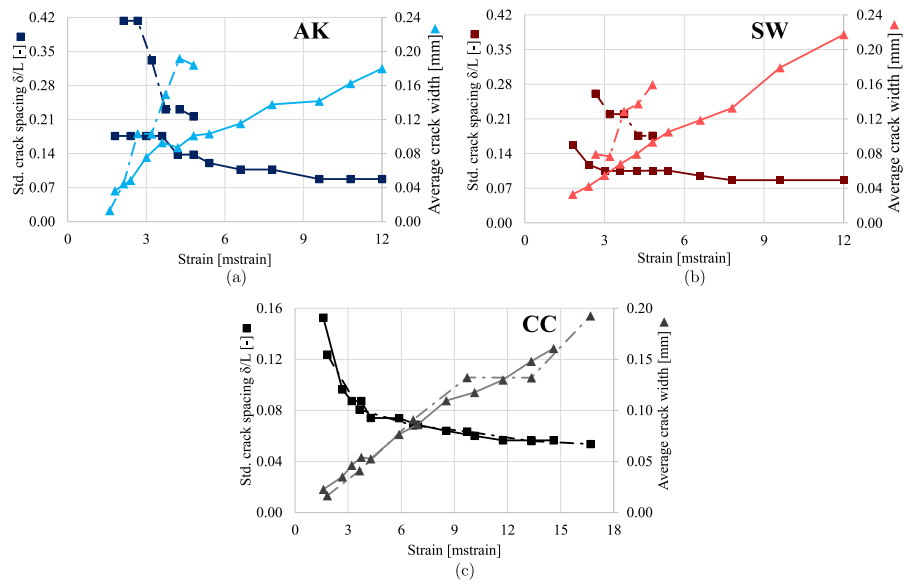


Figure 9: Crack pattern development during uni-axial traction for AK (a), SW (b) and CC (c) at 28-day (line-dot) and 60-day (solid) curing time. Crack spacing (left scale, triangles) and crack width (right scale, squares) is plotted vs strain

182 the control group for strength and strain. In contrast, long-term curing
 183 provides little benefit in the absence of aggressive attack.

184 • The crack pattern is a good indication of the degradation occurred in a
 185 composite. Interestingly, the limiting value at failure for the crack width
 186 seems to define the ultimate strength of the specimen and it appears char-
 187 acteristic of the composite as it is little sensitive to the aggressive envi-
 188 ronment and to the curing time (saturation crack width).

189 • The crack pattern *evolution* strongly depends on the aggressive environ-
 190 nment and on the curing time. In contrast, for the control group it is almost
 191 entirely independent on the curing time.

192 **Declarations of interest**

193 None.

194 **Acknowledgments**

195 Authors gratefully acknowledge financial support from Fondo di Ateneo per
 196 la Ricerca FAR2016.

197 **Bibliography**

- 198 [1] Lanzoni L, Nobili A, Tarantino AM. Performance evaluation of a
199 polypropylene-based draw-wired fibre for concrete structures. *Construction*
200 and *Building Materials*. 2012;28(1):798–806.
- 201 [2] Italian National Research Council (CNR) . Guide for the design and con-
202 struction of an externally bonded FRP system for strengthening existing
203 structures. DT200. 2004;.
- 204 [3] Nobili A, Signorini C. On the effect of curing time and environmental
205 exposure on impregnated Carbon Fabric Reinforced Cementitious Matrix
206 (CFRCM) composite with design considerations. *Composites Part B: En-*
207 *gineering*. 2017;112:300–313.
- 208 [4] ICC-Evaluation Service . Acceptance criteria for masonry and concrete
209 strengthening using fiber-reinforced cementitious matrix (FRCM) compos-
210 ite systems. AC434. 2013;. Whittier, CA.
- 211 [5] Technical Committee 232-TDT . Test methods and design of textile rein-
212 forced concrete. *Materials and Structures*. 2016;49(12):4923–4927.
- 213 [6] Signorini C, Nobili A, Gonzalez EI Cedillo, Siligardi C. Silica coating for
214 interphase bond enhancement of carbon and AR-glass Textile Reinforced
215 Mortar (TRM). *Composites Part B: Engineering*. 2018;.
- 216 [7] Arboleda D. Fabric Reinforced Cementitious Matrix (FRCM) Compos-
217 ites for Infrastructure Strengthening and Rehabilitation: Characterization
218 Methods. PhD thesis University of Miami 2014. Open Access Dissertation.
219 Paper 1282.
- 220 [8] Arboleda D, Babaeidarabad S, Hays CDL, Nanni A. Durability of Fab-
221 ric Reinforced Cementitious Matrix (FRCM) Composites. In: *CICE 2014;*
222 *2014. Vancouver, 20-22 August 2014.*
- 223 [9] Nobili A. Durability assessment of impregnated Glass Fabric Reinforced
224 Cementitious Matrix (GFRCM) composites in the alkaline and saline en-
225 vironments. *Construction and Building Materials*. 2016;105:465–471.
- 226 [10] Micelli F, Aiello MA. Residual tensile strength of dry and impregnated
227 reinforcement fibres after exposure to alkaline environments. *Composites*
228 *Part B: Engineering*. 2017;. available online.
- 229 [11] Butler M, Mechtcherine V, Hempel S. Experimental investigations on the
230 durability of fibre–matrix interfaces in textile-reinforced concrete. *Cement*
231 *and Concrete Composites*. 2009;31(4):221–231.
- 232 [12] Butler M, Mechtcherine V, Hempel S. Durability of textile reinforced con-
233 crete made with AR glass fibre: effect of the matrix composition. *Materials*
234 *and structures*. 2010;43(10):1351–1368.

- 235 [13] Hempel R, Butler M, Hempel S, Schorn H. Durability of textile reinforced
236 concrete. Special Publication. 2007;244:87–108.
- 237 [14] Mobasher B, Peled A, Pahilajani J. Distributed cracking and stiff-
238 ness degradation in fabric-cement composites. Materials and structures.
239 2006;39(3):317–331.
- 240 [15] Gebler SH, Jones CL, Brogna D, et al. Guide to curing concrete. In: ; 2001.
- 241 [16] American Concrete Institute . Recommended practice for curing concrete
242 (ACI 308m). ACI standard American Concrete Institute; 1998.
- 243 [17] Nobili A, Lanzoni L, Tarantino AM. Experimental investigation and mon-
244 itoring of a polypropylene-based fiber reinforced concrete road pavement.
245 Construction and Building Materials. 2013;47:888–895.
- 246 [18] Gowripalan N. Effect of curing on durability. Concrete International.
247 1990;12(2):47–54.
- 248 [19] Zhutovsky S, Kovler K. Effect of internal curing on durability-related
249 properties of high performance concrete. Cement and concrete research.
250 2012;42(1):20–26.
- 251 [20] Falope FO, Lanzoni L, Tarantino AM. Modified hinged beam test on steel
252 fabric reinforced cementitious matrix (SFRCM). Composites Part B: En-
253 gineering. 2018;In press.
- 254 [21] Mobasher B. Mechanics of fiber and textile reinforced cement composites.
255 CRC press; 2011.
- 256 [22] Lepech Michael, Li Victor C. Water permeability of cracked cementitious
257 composites. 2005;.
- 258 [23] Nobili A, Falope FO. Impregnated Carbon Fabric-Reinforced Cementitious
259 Matrix Composite for Rehabilitation of the Finale Emilia Hospital Roofs:
260 Case Study. Journal of composites for construction. 2017;:05017001.